Interaction between KDELR2 and HSP47 as a Key Determinant in Osteogenesis Imperfecta Caused by Bi-allelic Variants in *KDELR2*

Fleur S. van Dijk,[1,2,3,4,25,*] Oliver Semler,[5,6,25] Julia Etich,[7,25] Anna Köhler,[8] Juan A. Jimenez-Estrada,[9] Nathalie Bravenboer,[10] Lauria Claeys,[11] Elise Riesebos,[11] Sejla Gegic,[11] Sander R. Piersma,[12] Connie R. Jimenez,[12] Quinten Waisfisz,[11] Carmen-Lisset Flores,[9] Julian Nevado,[13,14] Arjan J. Harsevoort,[1] Guus J.M. Janus,[1] Anton A.M. Franken,[1] Astrid M. van der Sar,[15] Hanne Meijers-Heijboer,[11] Karen E. Heath,[13,14,16] Pablo Lapunzina,[13,14] Peter G.J. Nikkels,[17] Gijs W.E. Santen,[18] Julian Nüchel,[8] Markus Plomann,[8] Raimund Wagener,[8,19] Mirko Rehberg,[5] Heike Hoyer-Kuhn,[5] Elisabeth M.W. Eekhoff,[20] Gerard Pals,[11] Matthias Mörgelin,[21] Simon Newstead,[22] Brian T. Wilson,[3,23] Victor L. Ruiz-Perez,[9,13,14] Alessandra Maugeri,[11] Christian Netzer,[6,24] Frank Zaucke,[7,26] and Dimitra Micha[11,26,*]

Summary

Osteogenesis imperfecta (OI) is characterized primarily by susceptibility to fractures with or without bone deformation. OI is genetically heterogeneous: over 20 genetic causes are recognized. We identified bi-allelic pathogenic *KDELR2* variants as a cause of OI in four families. *KDELR2* encodes KDEL endoplasmic reticulum protein retention receptor 2, which recycles ER-resident proteins with a KDEL-like peptide from the *cis*-Golgi to the ER through COPI retrograde transport. Analysis of patient primary fibroblasts showed intracellular decrease of HSP47 and FKBP65 along with reduced procollagen type I in culture media. Electron microscopy identified an abnormal quality of secreted collagen fibrils with increased amount of HSP47 bound to monomeric and multimeric collagen molecules. Mapping the identified *KDELR2* variants onto the crystal structure of *G. gallus* KDELR2 indicated that these lead to an inactive receptor resulting in impaired KDELR2-mediated Golgi-ER transport. Therefore, in KDELR2-deficient individuals, OI most likely occurs because of the inability of HSP47 to bind KDELR2 and dissociate from collagen type I. Instead, HSP47 remains bound to collagen molecules extracellularly, disrupting fiber formation. This highlights the importance of intracellular recycling of ER-resident molecular chaperones for collagen type I and bone metabolism and a crucial role of HSP47 in the KDELR2-associated pathogenic mechanism leading to OI.

Osteogenesis imperfecta (OI) (MIM: PS166200) is a clinically and genetically heterogeneous connective tissue disorder characterized by liability to fractures with or without bone deformation. Secondary features include blue sclerae, dentinogenesis imperfecta (DI), progressive hearing loss, and joint hypermobility. OI is divided into five clinical types, and it has long been estimated that 90% of individuals with OI have dominant pathogenic variants in *COL1A1* (MIM: 120150) or *COL1A2* (MIM: 120160) encoding the α1 and α2 chains of collagen type I. However, there is growing evidence that autosomal-recessive forms of OI can be more common in consanguineous populations.[1,2] OI type 1 (MIM: 166200) is usually caused by pathogenic variants resulting in haploinsufficiency of *COL1A1*, and OI type 5 (MIM: 610967) is always caused by the dominant c.−14C>T variant in the 5′ UTR of *IFITM5*.[1] To date,

[1]Expert Center for Adults with Osteogenesis Imperfecta, Isala Hospital, 10400 Zwolle, the Netherlands; [2]Department of Clinical Genetics, University Medical Center Groningen, 30001 Groningen, the Netherlands; [3]North West Thames Regional Genetics Service, London North West Health Care University NHS Trust, Harrow HA1 3UJ, UK; [4]Department of Metabolism, Digestion and Reproduction, Section of Genetics and Genomics, Imperial College London, London, UK; [5]Department of Paediatrics, Faculty of Medicine and University Hospital Cologne, University of Cologne, Cologne 50931, Germany; [6]Center for Rare Diseases, University Hospital Cologne, University of Cologne, Cologne 50931, Germany; [7]Dr. Rolf M. Schwiete Research Unit for Osteoarthritis, Orthopaedic University Hospital Friedrichsheim gGmbH, Frankfurt/Main 60528, Germany; [8]Center for Biochemistry, Faculty of Medicine and University Hospital Cologne, University of Cologne, Cologne 50931, Germany; [9]Instituto de Investigaciones Biomédicas "Alberto Sols" (IIBM), CSIC-UAM, Madrid 28029, Spain; [10]Department of Clinical Chemistry, Amsterdam Movement Sciences, Amsterdam UMC, Vrije Universiteit Amsterdam, Amsterdam, the Netherlands; [11]Department of Clinical Genetics, Amsterdam UMC, Vrije Universiteit Amsterdam, Amsterdam 1081BT, the Netherlands; [12]Department of Medical Oncology, Cancer center Amsterdam, Amsterdam UMC, Vrije Universiteit Amsterdam, Amsterdam, the Netherlands; [13]Centro de Investigación Biomédica en Red Enfermedades Raras (CIBERER), ISCIII, Madrid 28029, Spain; [14]Institute of Medical & Molecular Genetics (INGEMM), Hospital Universitario La Paz-IdiPaz-Universidad Autonóma de Madrid, Madrid 28046, Spain; [15]Department of Medical Microbiology and Infection Control, Amsterdam UMC, Vrije Universiteit Amsterdam, Amsterdam, the Netherlands; [16]Skeletal Dysplasia Multidisciplinary Unit (UMDE), Hospital Universitario La Paz, Universidad Autonóma de Madrid, Madrid 28046, Spain; [17]Department of Pathology, University Medical Center Utrecht, Utrecht, the Netherlands; [18]Department of Clinical Genetics, Leiden University Medical Centre, Leiden, the Netherlands; [19]Center for Molecular Medicine Cologne, University of Cologne, Cologne 50931, Germany; [20]Department of Internal Medicine Section Endocrinology, Amsterdam Movement Sciences, Amsterdam UMC, Vrije Universiteit Amsterdam, Amsterdam, the Netherlands; [21]Colzyx AB, Medicon Village, Lund 22381, Sweden; [22]Department of Biochemistry, University of Oxford, South Parks Road, Oxford OX1 3QU, UK; [23]Biosciences Institute, Newcastle University, International Centre for Life, Newcastle upon Tyne NE1 3BZ, UK; [24]Institute of Human Genetics, Faculty of Medicine and University Hospital Cologne, University of Cologne, Cologne 50931, Germany
[25]These authors contributed equally
[26]These authors contributed equally
*Correspondence: fleur.dijk@nhs.net (F.S.v.D.), d.micha@amsterdamumc.nl (D.M.)
https://doi.org/10.1016/j.ajhg.2020.09.009.

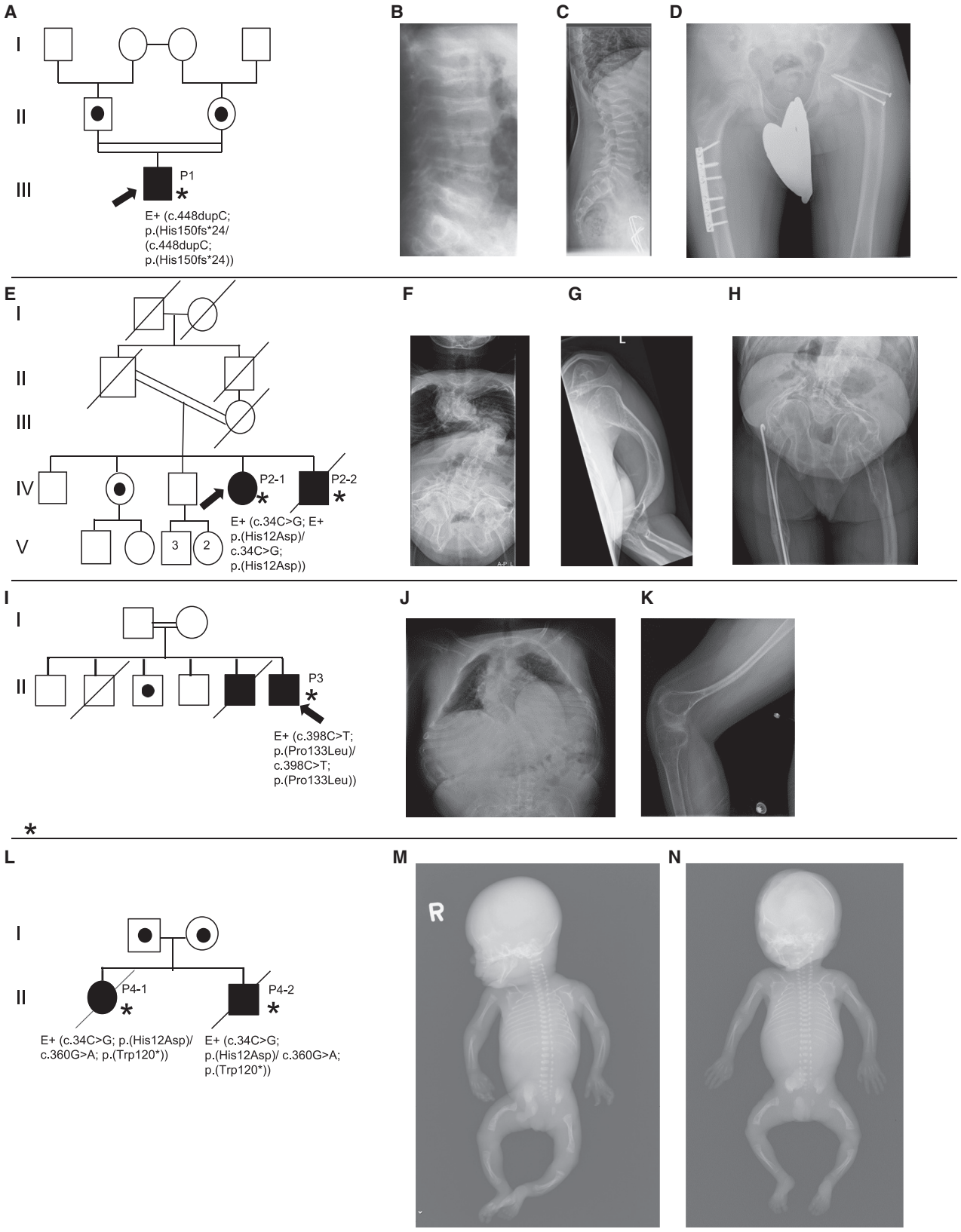

Figure 1. Pedigrees and Radiographs of P1 (A–D), P2-1 (E–H), P3 (I–K), and P4-1 and P4-2 (L–M)
(A) Pedigree of P1.
(B and C) Radiographs of the lateral spine at the start of bisphosphonate treatment and after 9 years of treatment. Only mild reshaping of the vertebrae is visible, demonstrating a limited effect of the antiresorptive treatment. Improvement of vertebral morphology is less than reported in the literature for individuals affected with OI.[6]

(legend continued on next page)

pathogenic changes in more than 20 different genes have been associated with clinical OI types 2–4 (MIM: 166210, 259420, 166220), monogenetic osteoporosis without extraskeletal features of OI, and syndromic or atypical OI. Many of these genes cluster into five functional groups based on the role of their gene product in bone structure or metabolism: (1) collagen type I primary structure, (2) collagen type I modification, (3) collagen type I processing and crosslinking, (4) osteoblast differentiation and function, and (5) bone mineralization and osteoclast function.[3,4] Dominant defects in the canonical WNT signaling pathway (*WNT1* [MIM: 164820] and *LRP5* [MIM: 603506]) cause osteoporosis without extraskeletal features of OI, whereas recessive defects in *LRP5* are associated with osteoporosis-pseudoglioma syndrome (MIM: 259770).[1] Description of recessive variants in *SEC24D* (MIM: 607186), causative of (atypical) OI and Cole-Carpenter syndrome (MIM: 616294) due to impaired anterograde COP (coat protein) II transport,[5] has introduced defects in intracellular trafficking as a novel mechanism in this group of disorders. Although many genetic causes for OI have been identified, there are still families in which the molecular defect remains unknown. Here, we describe six affected individuals from four families. Informed consent was obtained from each participant or family and institutional review board approval had been given for the study. All individuals (P1 [individual III-1 in Figure 1A], P2-1 [individual IV-3 in Figure 1E], P2-2 [individual IV-4 in Figure 1E], P3 [individual II-6 in Figure 1I], P4-1 [individual II-1 in Figure 1L], and P4-2 [individual II-2 in Figure 1L]) had been diagnosed with a clinical diagnosis of progressively deforming OI or OI type 2B/3. Physical examination was carried out in combination with radiological surveys. Individuals P1, P2-1, P2-2, and P3 had disproportionate short stature and experienced multiple fractures from early childhood leading to progressive skeletal deformation and requiring recurrent surgical interventions. In P2-1, P2-2, and P3, progression led to wheelchair dependence, in childhood for P2-1 and P2-2 and at 18 years for P3. No bisphosphonate therapy was available in childhood. In P1, low bone density was seen to improve with bisphosphonate therapy, and mobility was maintained at 12 years. P4-1 and P4-2 were detected during pregnancy. Ultrasound in early pregnancy showed a suspicion of a severe skeletal dysplasia, and both pregnancies were terminated at 24- and 22-weeks gestational age, respectively. The babygrams of both fetuses showed slender ribs and malformed bowed tibia and femur due to multiple fractures, compatible with OI type 2B/3. The clinical features of each affected individual are detailed in Table 1. Pedigrees and radiographs appear in Figure 1. Clinical reports are available in the Supplemental Information. For P1, P2-1, P3, and P4-1, next-generation sequencing (NGS) was used to interrogate a panel of genes known to be associated with OI and related disorders. Because no pathogenic variants were identified, a whole-exome sequencing (WES) approach was adopted for P1, P2-1, and P3. P1 was analyzed by singleton WES followed by Sanger sequencing of the consanguineous parents for the identified variant. Because the parents of P2-1 were deceased, she and her unaffected sister were sequenced in tandem, assuming autosomal-recessive inheritance in view of parental consanguinity and another affected sibling. In P3, WES was performed in combination with homozygosity mapping with a SNP array (Illumina Cyto850K Beadchip). In family 4, whole-genome sequencing (WGS) was performed on P4-1 as a single case. Subsequently, a panel of 35 OI-related genes was analyzed. P4-2 was tested for identified variants by Sanger sequencing (Supplemental Information).

P1–P3 were found to have homozygous variants in *KDELR2* (GenBank: NM_006854.3). P1 has a c.448dupC (p.His150fs*24) frameshift variant, P2-1 and P2-2 have a c.34C>G (p.His12Asp) missense variant, and P3 has a c.398C>T (p.Pro133Leu) missense variant. P4-1 and P4-2 both showed compound heterozygosity for the variants c.34C>G (p.His12Asp) and c.360G>A (p.Trp120*). None of these variants are present in the gnomAD. The two missense variants affect highly conserved amino acids and are predicted to be pathogenic via *in silico* prediction analysis (CADD V1.4, DANN, MutationTaster, PolyPhen). All variants were verified by Sanger sequencing. In addition, the unaffected parents of P1 were confirmed to be heterozygous for the c.448dupC (p.His150fs*24) variant. One unaffected sister of P2-1 and P2-2 was heterozygous for the c.34C>G (p.His12Asp) variant, and sequence analysis of the c.398C>T (p.Pro133Leu) variant in three

(D) Radiograph of pelvis and both femurs after surgical procedures to stabilize fractures. Right femur is supported by a plate to stabilize the femur shaft fracture, and on the left side, screws have been used to treat a femoral neck fracture. Both femurs demonstrate good differentiation between cortical and trabecular bone with a relatively thick cortex contrary to the severely compressed vertebrae.
(E) Pedigree of P2-1; asterisk denotes the number of sons/daughters.
(F) Severe left convex scoliosis measuring 80 degrees at the lumbar level and 116 degrees at the thoracic level.
(G) Deformation of the left shoulder with severe bowing of the left arm.
(H) Deformed pelvis with bilateral protrusio acetabulum.
(I) Pedigree of P3.
(J) Barrel shaped thorax, dorsal scoliosis, and loss of height of the vertebral bodies; osteopenia.
(K) Slender and curved diaphysis of the femur and fibula; osteopenia and muscular atrophy.
(L) Pedigree of P4-1 and P4-2.
(M and N) Babygrams of P4-1 and P4-2 at 24 weeks and 22+1 weeks of pregnancy, respectively, showed normal ossification of the skull and normal shape of the long bones of the upper extremity. The ribs were slender but showed no fractures. The long bones of the lower extremity were malformed because of multiple fractures, and both femora were more severely affected. A radiological diagnosis of OI type 2B/3 was made.
E, a clinical diagnosis of OI type 2B/3; asterisk, documented evaluation.

Table 1. Clinical and Radiological Features of P1, P2-1, P3, P4-1, and P4-2

Individual	P1	P2-1	P2-2[a]	P3	P4-1	P4-2
Ethnicity	**Pakistani**	**Dutch**	**Dutch**	**Spanish**	**Dutch**	**Dutch**
Genetic cause	c.448dupC (p.His150fs*24), homozygous	c.34C>G (p.His12Asp), homozygous	N/A	c.398C>T (p.Pro133Leu), homozygous	c.34C>G (p.His12Asp), c.360G>A (p.Trp120*)	c.34C>G (p.His12Asp), c.360G>A (p.Trp120*)
Age, first assessment	5 years	29 years	N/A	1.5 months	24 weeks of gestation	N/A
Age, last assessment	14 years	39 years	N/A	43 years	N/A	N/A
Height, last assessment	130 cm	121 cm	115 cm	138 cm	N/A	N/A
Confirmed prenatal fractures	–	–	–	–	+	+
Wormian bones	–	U	U	+	N/A	N/A
Age at first fracture (months)	40	32	U	24	*in utero*	*in utero*
Estimated number of sustained fractures	N = 12	N = 26	N = 15 aged 25 years	N > 30	N/A	N/A
Last sustained fracture	right femur age 10 years	right femur age 28 and right femoral neck age 29	U	right femur, age 37	N/A	N/A
Color of sclera	white	white	white	white	U	U
Dentinogenesis imperfecta	–	–	–	–	N/A	N/A
Hypermobility of joints	+	+	U	+	N/A	N/A
Hearing impairment	–	–	–	–	N/A	N/A
Chest deformity	barrel shaped with pectus excavatum	barrel shaped with pectus excavatum	+	bell shaped	–	–
Cardiac abnormalities	–	–	+	U	–	–
Vertebral fractures[b]	+	+	U	+	N/A	N/A
Scoliosis	–	+	+	+	–	–
Bowing of upper extremities[b]	–	+	+	+	–	–
Bowing of lower extremities[b]	–	+	+	+	+	+
Shortening of upper extremities[b]	–	+	+	+	+	+
Shortening of lower extremities[b]	–	+	+	+	+	+
Surgical correction for bone deformation	+	+	+	+	N/A	N/A
Age at BP treatment (start/end)	5/9 years	29/37 years	N/A	39/42 years	N/A	N/A
BP type and dosage	neridronate 2 mg/kg body weight, IV, every 3 months	alendronic acid 70 mg, weekly	N/A	zoledronate 5 mg, IV, yearly	N/A	N/A
DEXA scores before BP treatment	*Z* score: *L2–L4, −3.7; * TBLH, −1.9	*Z* score: *L2–L4, −3.09; *femoral neck (R), −2.05; *trochanter, −2.50	N/A	U: severe osteoporosis on X-rays	N/A	N/A
DEXA scores after BP treatment	*Z* score: *L2–L4, −2.4	Z-score: *L1–L4, −3.4	N/A	U	N/A	N/A

(*Continued on next page*)

Table 1. ***Continued***

Individual	P1	P2-1	P2-2[a]	P3	P4-1	P4-2
Ethnicity	**Pakistani**	**Dutch**	**Dutch**	**Spanish**	**Dutch**	**Dutch**
Mobility	mobile	wheelchair since age of 4.5 years	wheelchair	wheelchair since age of 18 years	N/A	N/A
Intelligence	normal	normal	normal	normal	N/A	N/A
Calcium – level (mmol/L)[b]	2.36	2.55	U	2.49	N/A	N/A
Alkaline phosphatase at first visit (U/L)	201	69	U	U	N/A	N/A
Alkaline phosphatase at last visit (U/L)	198	56	U	U	N/A	N/A

Abbreviations are as follows: U, unknown; N/A, not applicable; BP, bisphosphonate; TBLH, total body less head.
[a]P2-2 passed away at the age of 35 years.
[b]At first presentation.

available unaffected siblings of P3 identified two with normal sequence and one with the variant in the heterozygous state.

KDELR2 is a member of the KDEL receptor family (KDELR1, KDELR2, KDELR3), which consists of seven transmembrane (TM) domains organized into two triple helix bundles separated by a linking domain (TM4). The KDEL receptors localize mainly to the Golgi-complex (usually *cis*-side), the endoplasmic reticulum (ER), and the intermediate ER-Golgi compartment (ERGIC).[7] An important function of KDELRs is to regulate the trafficking of proteins between the Golgi apparatus and the ER, aiming to return soluble ER-resident proteins back to the ER from the intermediate compartment of *cis*-Golgi. ER luminal proteins that are recognized by KDEL receptors harbor a C-terminal Lys-Asp-Glu-Leu (KDEL)-like motif. A polar cavity responsible for pH-dependent KDEL sequence recognition is formed at the luminal surface of the receptor. Binding of proteins displaying a C-terminal KDEL-like motif occurs in acidic conditions and induces a conformational change in the cytoplasmic aspect of the protein, exposing a dilysine-like retrieval motif required for transport to the ER by COPI vesicles. On arrival at the ER, the higher pH environment results in dissociation of the KDEL-motif-bearing protein from the KDEL receptor, which is then recycled to the Golgi by COPII vesicles.[7,8]

Dermal fibroblasts were available for analysis from individuals P1 and P2-1 and in a later stage from P3. As shown by quantitative PCR analysis, the expression of *KDELR2* was severely decreased in fibroblasts of P1 with the homozygous frameshift variant p.His150fs (c.448dupC) and almost unchanged in P2-1 with the homozygous missense variant p.His12Asp (c.34C>G) compared to fibroblasts from healthy donors (Figure 2A). Although highly conserved, the human KDELRs display different substrate affinities, e.g., KDELR2 binds HDEL motifs more readily than KDELR1/3.[9] Defects in individual KDELRs are therefore unlikely to be rescued through functional redundancy with other members of the family. Our results indeed showed no evidence for a potential compensatory upregulation of *KDELR1/3* in fibroblasts of individuals with biallelic *KDELR2* variants (Figure 2A).

We first tested collagen secretion in fibroblasts from controls or P1 (p.His150fs) and P2-1 (p.His12Asp). Using non-quantitative immunofluorescence analysis, we observed a variable extent of intracellular procollagen type I in fibroblasts from control and affected individuals that was more apparent at day 1, when cells initiate the secretion of large amounts of extracellular matrix. The signal intensity of intracellular procollagen type I appeared increased in individual fibroblasts of P1 (p.His150fs) and P2-1 (p.His12Asp), suggesting a delayed secretion (Figure 2B, denoted by asterisks). In addition, a reduced amount of secreted collagen type I in the cell culture media could be observed (Figure 2C), leading to the assumption that intracellular collagen might be retained. This intracellular procollagen type I partially colocalized with the ER-marker PDI in all cell populations (Figure S1A), indicating that a proportion of procollagen type I is indeed found within the ER. However, by quantitative densitometric analysis of immunoblots, we could not detect increased amounts of intracellular procollagen type I in cell extracts from entire cultures (Figures S3B and S3C). Instead, we observed a 2.2-fold and a 1.7-fold reduction of collagen gene expression in fibroblasts of P1 (p.His150fs) and P2-1 (p.His12Asp), respectively (Figure S1D), which might in part account for the reduced amount of secreted collagen type I.

ER-resident collagen chaperones that are transported through their KDEL-like ER retention signal are crucial for proper collagen secretion from the ER. No changes were found in the amount of ER-resident proteins P3H1 (Figure 3A, Figure S1D) and CYPB (data not shown) in cells from affected individuals. Consistent with these findings, α1(I) P986 3-hydroxylation, which has been shown to be decreased in individuals with deficiency of CRTAP (MIM: 605497), P3H1 (MIM: 610339),[10] or CYPB (MIM: 123841),[11] was not decreased compared to healthy donors (Figure S2C and S3). Although the transcriptional

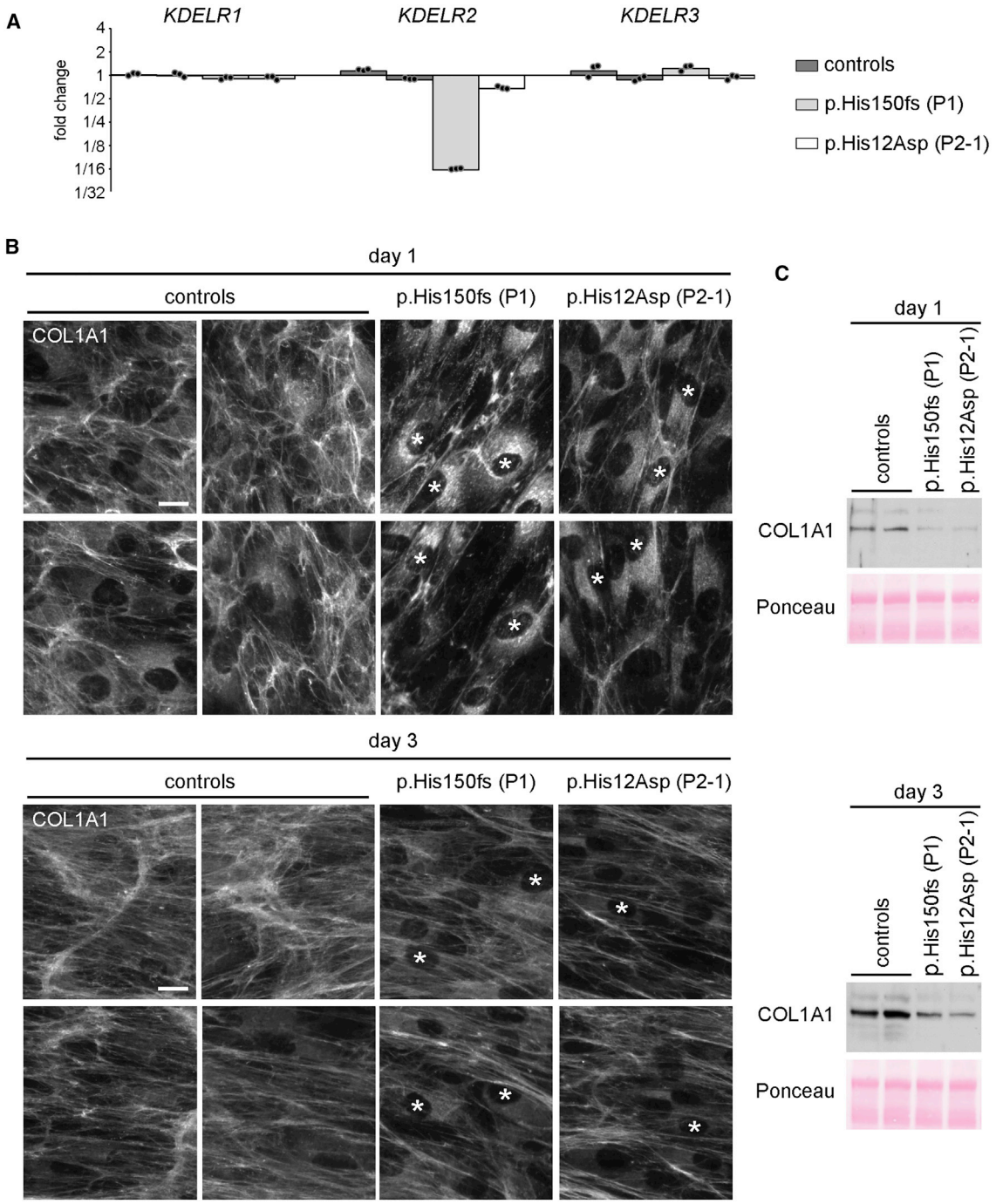

Figure 2. *KDELR2* Variants in P1 and P2-1 Lead to Retention of Collagen Type I in Cultured Fibroblasts without Compensating Effects of *KDELR1* and *KDELR3*

(A) Expression of *KDELR1*, *KDELR2*, and *KDELR3* in cultured fibroblasts was normalized to *GAPDH* and log2-transformed. For better visualization, corresponding fold changes are displayed on a log2-transformed axis for controls and fibroblasts derived from affected individuals (P1 [p.His150fs] and P2-1 [p.His12Asp]). Individual values and the mean of technical replicates are given.

(B) Collagen type I protein (COL1) was detected in cultured fibroblasts by immunofluorescence microscopy after 1 or 3 days in different areas of the same culture. The brightness and contrast of fluorescent images was adjusted for visualization. Representative pictures are shown. Scale bar represents 20 μm.

(C) Soluble fraction of COL1 in the supernatant of cultured confluent fibroblasts was detected by immunoblotting after 1 and 3 days. Ponceau S staining was used as loading control.

expression of the ER-resident chaperones HSP47 (encoded by *SERPINH1*) and FKBP65 (encoded by *FKBP10*) was almost unchanged between affected individuals and healthy controls (Figure S1D), fibroblasts from affected individuals showed a decreased amount of intracellular HSP47 (Figure 3A) and FKBP65 (Figure 3B).

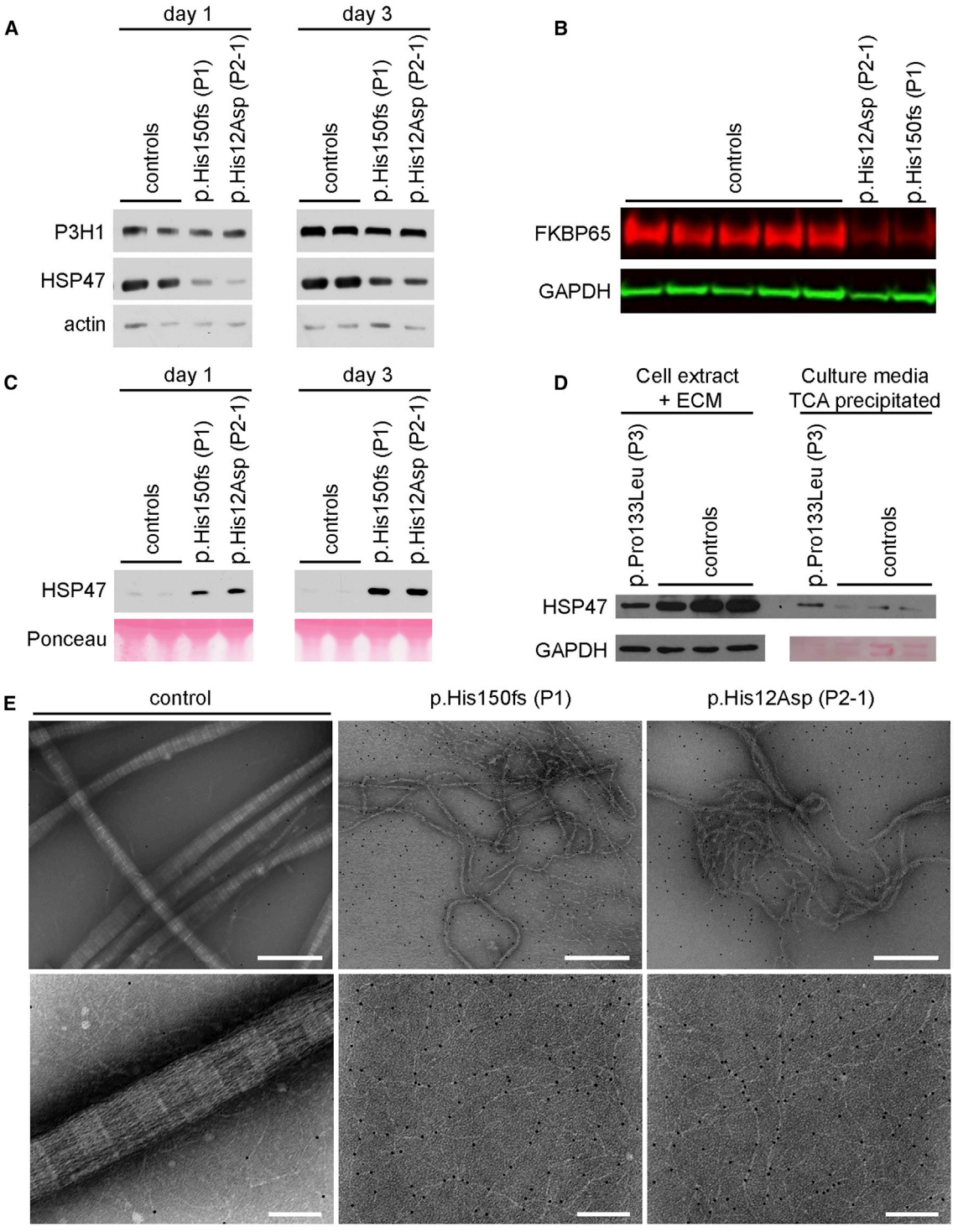

Figure 3. Mutations in *KDELR2* in Fibroblasts Derived from Affected Individuals Result in Reduction of HSP47 and FKBP65 Accompanied by Reduced Collagen Assembly and Quality due to Mislocalization of HSP47

(A) The protein amount of P3H1 and HSP47 in trypsinized fibroblasts was determined by immunoblotting on day 1 or day 3 in controls and fibroblasts derived from P1 (p.His150fs) and P2-1 (p.His12Asp). Detection of β-actin was used as loading control.

(B) The amount of FKBP65 in cultured control and fibroblasts derived from P1 (p.His150fs) and P2-1 (p.His12Asp) on day 1 were examined by immunoblotting. GAPDH was used to control equal protein loading.

(C) The protein amount of HSP47 in the supernatant of fibroblasts was determined by immunoblotting on day 1 and day 3 in controls and fibroblasts derived from P1 (p.His150fs) and P2-1 (p.His12Asp). Ponceau S staining was used as loading control.

(D) Representative immunoblot showing HSP47 amounts in the cell layer and supernatant of cultured control and fibroblasts derived from P3 (p.Pro133Leu). GAPDH amounts and Ponceau S staining served as loading control.

(E) Negative staining EM and TEM were used to visualize triple helical collagen and maturing collagen fibrils, whereas immunogold EM was used to detect localization of HSP47 in the supernatant of cultured control and fibroblasts derived from P1 (p.His150fs) and P2-1

(legend continued on next page)

Both HSP47 and FKBP65 have a KDEL-like signal at their C terminus, RDEL and HEEL, respectively, for which KDELR2 has been described to have specificity.[8] Reduced amounts and/or abnormal activity of HSP47 have been reported to influence the amounts of FKBP65.[12,13] In OI fibroblasts with a homozygous missense variant in *SERPINH1* leading to reduction of HSP47, a decrease in FKBP65 was observed, but not vice versa.[12] Thus, intracellular reduction of FKBP65 amounts in KDELR2-deficient cells might have been caused by reduced HSP47 amounts. HSP47 and FKBP65 are ER-resident chaperones that have been suggested to act together in collagen type I biosynthesis downstream of the 3-hydroxylation by the CRTAP/CYPB/P3H1 complex of the single P986 residue in the α1 chains of procollagen type I.[12,13] Pathogenic variants in *SERPINH1* and *FKBP10* have been reported to cause progressively deforming OI and Bruck syndrome 2/progressively deforming OI, respectively.[14,15] Fibroblasts of individuals with pathogenic *SERPINH1* or *FKBP10* mutations produce collagen chains of normal electrophoretic mobility,[14,15] and accordingly, collagen type I from fibroblasts of P1 (p.His150fs) and P2-1 (p.His12Asp) was pepsin-resistant and showed a normal electrophoresis pattern (Figures S2A and S2B and 2C). Interestingly, in cells of individuals with a pathogenic homozygous missense variant in *SERPINH1* encoding HSP47, "slightly delayed overall transit time from the ER to the extracellular space of collagen" was observed, although no obvious retention could be detected.[14]

In addition to FKBP65, HSP47 is known to interact in the cell with other proteins (e.g., TANGO1 and LH2), many of whom contribute to key steps in collagen regulation and function, including helix stability, telopeptide hydroxylation, collagen secretion, and matrix assembly,[16] and failure to recycle HSP47 to the ER may influence these key steps. Further investigations are necessary to elucidate the precise consequences of deficient KDELR2-dependent retrograde transport due to bi-allelic pathogenic *KDELR2* variants on these processes.

To assess the impact of *KDELR2* variants on general retrograde transport, we treated cells with Brefeldin A to block membrane transport out of but not back to the ER.[17] The Golgi protein GM130 was rapidly redistributed throughout the ER of control fibroblasts when treated with Brefeldin A for 15 min (Figure S4A). Assessment 60 min after removal of Brefeldin showed that the morphology of the Golgi apparatus was partially re-established. The steady-state distribution of GM130 was similarly altered in fibroblasts of P1 (p.His150fs) and P2-1 (p.His12Asp), indicating that neither the general Golgi-to-ER transport in cells of affected individuals in which KDELR1 and KDELR3 are unaffected nor retrieval of ER membrane proteins is impaired. In addition, previous reports have shown that KDELR2 triggers the Src signaling pathway to balance the membrane flux between ER and Golgi compartments and to regulate KDELR1- and KDELR2-dependent extracellular matrix degradation and invadopodia formation in cancer cells.[18,19] In primary fibroblasts from P1 (p.His150fs) and P2-1 (p.His12Asp), no obvious reduction of Src phosphorylation could be detected by immunoblot analysis compared to controls (Figure S4B). Other functions of the KDEL receptors were previously described and include participation in the ER stress response, specifically a role in the regulation of ER quality control.[7] However, our data showed a lack of aberrant cellular stress levels and response in fibroblasts of P1 and P2-1. We could not detect differences in the expression of the ER-resident KDEL-motif-containing PDI/P4HB (in which heterozygous mutations have been reported to cause Cole-Carpenter syndrome[5]) and the Golgi-resident Giantin (Figure S5A) or the expression of the ER stress-induced chaperone calnexin (data not shown). Time- and dose-dependent stimulation of cells of affected individuals with the ER stress inducers tunicamycin and thapsigargin also showed no differences in the expression of the ER stress markers *HSPA5* and *DDIT3* (Figures S5B and S5C). These results indicate that the impact of identified KDELR2 variants on these general processes is rather small and that KDELR2 must have another essential role in bone metabolism.

Interestingly, HSP47 was found to be secreted in the cell culture media in P1 and P2-1 (Figure 3C) and this was independently confirmed in P3 (Figure 3D). This abnormal secretion presumably accounts for the reduced amounts of intracellular HSP47. HSP47 normally associates transiently with procollagen molecules in the ER, aiding formation of the collagen triple helix for export to extracellular matrix by preventing unregulated aggregation of these molecules. HSP47 is thought to dissociate from these proteins under low pH conditions in the Golgi apparatus to be recycled to the ER.[20,21] Our data demonstrate that this is an active process dependent upon the ability of KDELR2 to bind HSP47, and KDELR2 is essential for recycling HSP47 back to the ER. Failure of HSP47 to dissociate from collagen may result in these molecules' being exported in complex. Secretion of HSP47 in affected individuals points to the inability of KDELR2 variants to recycle HSP47 back to the ER. To analyze whether secreted HSP47 does interfere with collagen fibril assembly, the structure of the secreted collagen fibrils in human fibroblast supernatants and the location of HSP47 molecules were analyzed by negative staining, immunogold detection, and transmission electron microscopy as described previously.[22,23] Specimens were labeled with antibodies directed against human HSP47. Immunogold staining revealed that this secreted HSP47 was bound to monomeric and multimeric collagen molecules (Figure 3E). In addition, collagen in controls was able to fold into banded collagen fibers, whereas the collagen fibrils in the cell culture media of fibroblasts of affected individuals remained

(p.His12Asp) after 3 days. Representative pictures are shown as overviews (upper panel) or higher magnification of diluted samples (lower panel). Scale bars represent 250 nm (upper panel), 100 nm (lower panel).

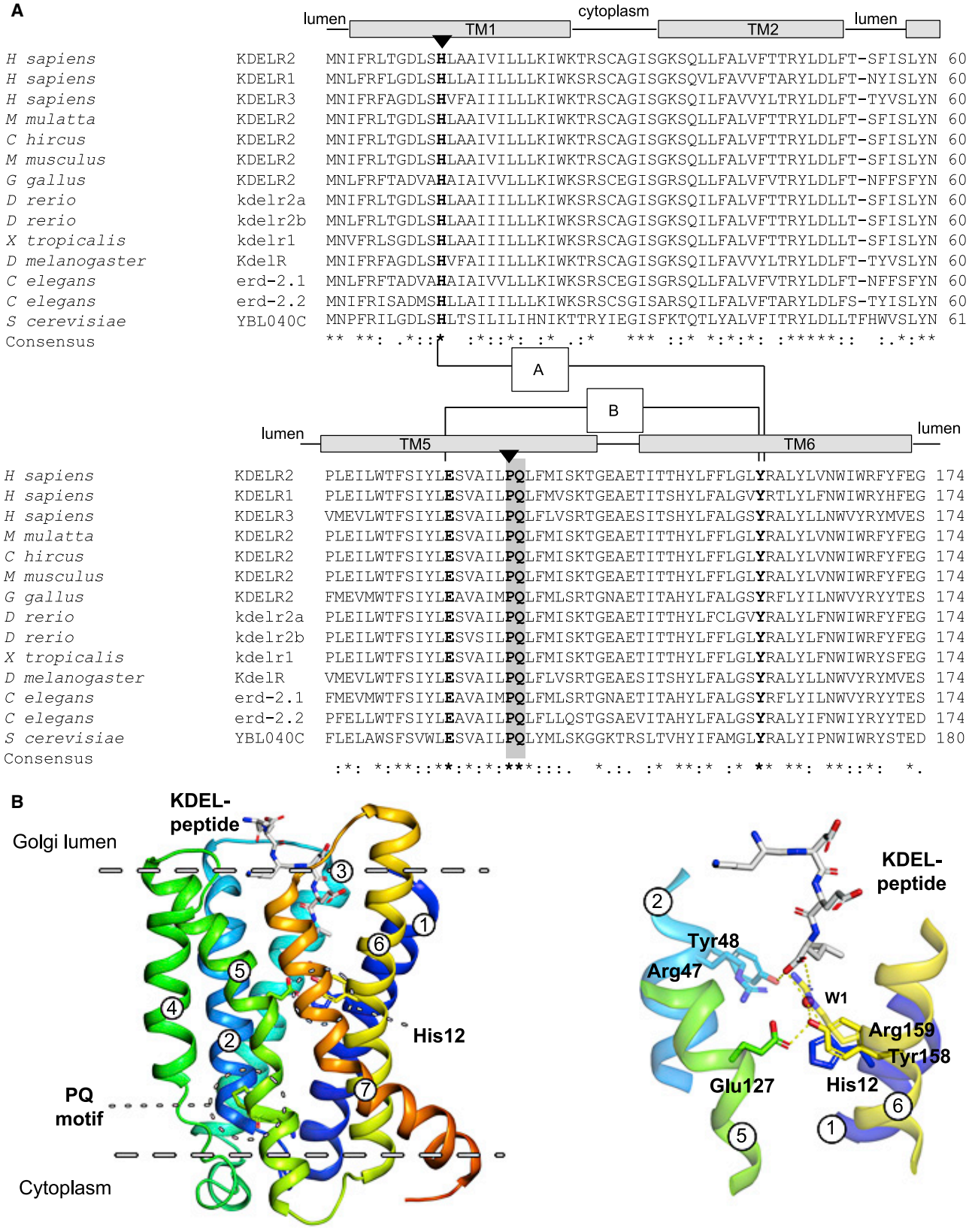

Figure 4. Evolutionary Conservation of KDELR Members of the PQ-Loop Motif Superfamily

(A) KDELR2 residues substituted in affected individuals (black triangles) are identical from yeast to man. Transmembrane regions are shown above the amino acid sequences. His12 and Tyr158 (box A) co-operate to coordinate the KDEL ligand of target proteins in a polar binding cavity. A short hydrogen bond between p.Glu127 and p.Tyr158 (box B) lock this in place. The PQ-loop motif for which the superfamily is named is colored gray.

(legend continued on next page)

thin and imperfectly folded. It has already been shown that HSP47 is an effective inhibitor of collagen fibril formation *in vitro* at neutral pH.[24] The role of HSP47 in preventing collagen aggregation, although an advantage for triple helix assembly in the Golgi, may therefore be responsible for failure of extracellular collagen fibril formation in all affected individuals reported here, and interference with fiber formation is likely to play a major role in the pathogenesis.

The question regarding how bi-allelic missense variants can cause an identical clinical phenotype as the bi-allelic frameshift variants resulting in reduction of KDELR2 remained. Members of the KDELR family demonstrate a high degree of evolutionary conservation (Figure 4A). Both residues mutated in P2-1 and P3 (c.398C>T [p.(Pro133Leu]) are identical from yeast to man. Recent crystal structures of the *G. gallus* KDELR2[24] reveal that the C terminus of the KDEL peptide interacts with His12 and Tyr158 through a water molecule, which is situated at the base of the peptide binding site. The conformational changes induced by KDEL peptide binding are stabilized through the formation of a short hydrogen bond between Glu127 and Tyr158, which locks the peptide within the receptor through interaction with Arg159. Substitution of the positively charged His12 for the negatively charged Asp is predicted to prevent KDEL peptide binding. Indeed, a p.His12Ala variant of the KDEL receptor resulted in complete loss of KDEL peptide binding *in vitro* and *in vivo*.[24] Because KDELR2 translocation to the ER is dependent upon exposure of the dilysine-like retrieval sequence, following peptide binding, the p.His12Ala mutant protein would be unable to recognize cargo or translocate to the ER, i.e., the same net effect as absence of KDELR2. The KDELR family is part of the PQ-loop protein superfamily,[25] characterized by a PQ-loop motif, which introduces a distinctive kink into TM5; in the KDEL receptor, this motif appears to play an important role in the positioning of Glu127 (Figure 4B). Pro133 is part of the KDELR2 PQ-loop motif; mutation to the amino acid Leu is predicted to remove the structurally important kink in TM5, repositioning Glu127 and preventing formation of the short hydrogen bond between this residue and Tyr158, which is required to stabilize KDEL peptide binding. The p.Pro133Leu variant is therefore also predicted to have a similar effect on KDELR2 function as p.His12Asp.

In summary, in four families with progressively deforming OI, recessive variants in *KDELR2*,consisting of one homozygous frameshift variant, two different homozygous missense variants, and a compound heterozygous nonsense and missense variant, were identified. On the basis of recently published crystal structures of chicken KDELR2 in signal peptide-free and peptide-bound states, the homozygous missense and frameshift *KDELR2* variants result in the same net effect: inability of KDELR2 to pick up cargo or translocate to the ER. Our experiments show (1) intracellular decrease of HSP47 and FKBP65 (both bearing KDEL-like motifs) and (2) reduced amount in culture media of procollagen type I in combination with (3) abnormal quality of secreted collagen type I with extracellular HSP47 bound to monomeric and multimeric collagen. Our results demonstrate defects in KDELR2 that lead to impaired KDELR2-dependent retrograde transport, resulting in a progressively deforming OI phenotype. In addition, we provide evidence for a crucial role of HSP47 in the pathogenic mechanism leading to OI because it appears bound to the collagen molecules extracellularly, most likely disrupting fiber formation. In the cell, HSP47 is known to interact with many other proteins contributing to collagen regulation and function. Failure to recycle HSP47 to the ER may therefore influence these interactions. Although further elucidation of the precise chain of events leading to OI is necessary, impaired KDELR2-mediated retrograde Golgi-to-ER transport can be considered another pathogenic mechanism in OI. This discovery highlights the importance of intracellular HSP47 retrograde trafficking in bone metabolism.

Data and Code Availability

The datasets supporting the conclusions of this article are included within the article and its additional file.

Supplemental Data

Supplemental Data can be found online at https://doi.org/10.1016/j.ajhg.2020.09.009.

Acknowledgments

We thank the affected individuals and their families for their kind cooperation. For the complete Acknowledgments, please see the Supplemental Acknowledgments.

Declaration of Interests

The authors declare no competing interests.

Received: February 15, 2020
Accepted: September 22, 2020
Published: October 13, 2020

Web Resources

GnomAD, http://gnomad-old.broadinstitute.org/
OMIM, https://omim.org/

(B) The crystal structure of *G. gallus* KDELR2 (PDB: 6I6H; colored N-term blue to C-term orange) bound to the TAEKDEL peptide (gray). The PQ-motif and His12 side chain are highlighted. On the right is a close-up view of the peptide binding site, showing the main interacting side chains. Hydrogen bond interactions are shown as yellow dashed lines. The water molecule (W1) linking the C terminus of the peptide with His12 is shown as a red sphere.

References

1. Van Dijk, F.S., and Sillence, D.O. (2014). Osteogenesis imperfecta: clinical diagnosis, nomenclature and severity assessment. Am. J. Med. Genet. A. *164A*, 1470–1481.
2. Essawi, O., Symoens, S., Fannana, M., Darwish, M., Farraj, M., Willaert, A., Essawi, T., Callewaert, B., De Paepe, A., Malfait, F., and Coucke, P.J. (2018). Genetic analysis of osteogenesis imperfecta in the Palestinian population: molecular screening of 49 affected families. Mol. Genet. Genomic Med. *6*, 15–26.
3. Forlino, A., and Marini, J.C. (2016). Osteogenesis imperfecta. Lancet *387*, 1657–1671.
4. Kang, H., Aryal A C, S., and Marini, J.C. (2017). Osteogenesis imperfecta: new genes reveal novel mechanisms in bone dysplasia. Transl. Res. *181*, 27–48.
5. Garbes, L., Kim, K., Rieß, A., Hoyer-Kuhn, H., Beleggia, F., Bevot, A., Kim, M.J., Huh, Y.H., Kweon, H.S., Savarirayan, R., et al. (2015). Mutations in SEC24D, encoding a component of the COPII machinery, cause a syndromic form of osteogenesis imperfecta. Am. J. Hum. Genet. *96*, 432–439.
6. Land, C., Rauch, F., Munns, C.F., Sahebjam, S., and Glorieux, F.H. (2006). Vertebral morphometry in children and adolescents with osteogenesis imperfecta: effect of intravenous pamidronate treatment. Bone *39*, 901–906.
7. Capitani, M., and Sallese, M. (2009). The KDEL receptor: new functions for an old protein. FEBS Lett. *583*, 3863–3871.
8. Kokubun, H., Jin, H., and Aoe, T. (2019). Pathogenic Effects of Impaired Retrieval between the Endoplasmic Reticulum and Golgi Complex. Int. J. Mol. Sci. *20*, 5614.
9. Raykhel, I., Alanen, H., Salo, K., Jurvansuu, J., Nguyen, V.D., Latva-Ranta, M., and Ruddock, L. (2007). A molecular specificity code for the three mammalian KDEL receptors. J. Cell Biol. *179*, 1193–1204.
10. Marini, J.C., Cabral, W.A., Barnes, A.M., and Chang, W. (2007). Components of the collagen prolyl 3-hydroxylation complex are crucial for normal bone development. Cell Cycle *6*, 1675–1681.
11. van Dijk, F.S., Nesbitt, I.M., Zwikstra, E.H., Nikkels, P.G., Piersma, S.R., Fratantoni, S.A., Jimenez, C.R., Huizer, M., Morsman, A.C., Cobben, J.M., et al. (2009). PPIB mutations cause severe osteogenesis imperfecta. Am. J. Hum. Genet. *85*, 521–527.
12. Duran, I., Nevarez, L., Sarukhanov, A., Wu, S., Lee, K., Krejci, P., Weis, M., Eyre, D., Krakow, D., and Cohn, D.H. (2015). HSP47 and FKBP65 cooperate in the synthesis of type I procollagen. Hum. Mol. Genet. *24*, 1918–1928.
13. Ishikawa, Y., Holden, P., and Bächinger, H.P. (2017). Heat shock protein 47 and 65-kDa FK506-binding protein weakly but synergistically interact during collagen folding in the endoplasmic reticulum. J. Biol. Chem. *292*, 17216–17224.
14. Christiansen, H.E., Schwarze, U., Pyott, S.M., AlSwaid, A., Al Balwi, M., Alrasheed, S., Pepin, M.G., Weis, M.A., Eyre, D.R., and Byers, P.H. (2010). Homozygosity for a missense mutation in SERPINH1, which encodes the collagen chaperone protein HSP47, results in severe recessive osteogenesis imperfecta. Am. J. Hum. Genet. *86*, 389–398.
15. Schwarze, U., Cundy, T., Pyott, S.M., Christiansen, H.E., Hegde, M.R., Bank, R.A., Pals, G., Ankala, A., Conneely, K., Seaver, L., et al. (2013). Mutations in FKBP10, which result in Bruck syndrome and recessive forms of osteogenesis imperfecta, inhibit the hydroxylation of telopeptide lysines in bone collagen. Hum. Mol. Genet. *22*, 1–17.
16. Oecal, S., Socher, E., Uthoff, M., Ernst, C., Zaucke, F., Sticht, H., Baumann, U., and Gebauer, J.M. (2016). The pH-dependent Client Release from the Collagen-specific Chaperone HSP47 Is Triggered by a Tandem Histidine Pair. J. Biol. Chem. *291*, 12612–12626.
17. Lippincott-Schwartz, J., Yuan, L.C., Bonifacino, J.S., and Klausner, R.D. (1989). Rapid redistribution of Golgi proteins into the ER in cells treated with brefeldin A: evidence for membrane cycling from Golgi to ER. Cell *56*, 801–813.
18. Pulvirenti, T., Giannotta, M., Capestrano, M., Capitani, M., Pisanu, A., Polishchuk, R.S., San Pietro, E., Beznoussenko, G.V., Mironov, A.A., Turacchio, G., et al. (2008). A traffic-activated Golgi-based signalling circuit coordinates the secretory pathway. Nat. Cell Biol. *10*, 912–922.
19. Ruggiero, C., Fragassi, G., Grossi, M., Picciani, B., Di Martino, R., Capitani, M., Buccione, R., Luini, A., and Sallese, M. (2015). A Golgi-based KDELR-dependent signalling pathway controls extracellular matrix degradation. Oncotarget *6*, 3375–3393.
20. Ito, S., and Nagata, K. (2019). Roles of the endoplasmic reticulum-resident, collagen-specific molecular chaperone Hsp47 in vertebrate cells and human disease. J. Biol. Chem. *294*, 2133–2141.
21. Besio, R., Chow, C.W., Tonelli, F., Marini, J.C., and Forlino, A. (2019). Bone biology: insights from osteogenesis imperfecta and related rare fragility syndromes. FEBS J. *286*, 3033–3056.
22. Engel, J., and Furthmayr, H. (1987). Electron microscopy and other physical methods for the characterization of extracellular matrix components: laminin, fibronectin, collagen IV, collagen VI, and proteoglycans. Methods Enzymol. *145*, 3–78.
23. Köhler, A., Mörgelin, M., Gebauer, J.M., Öcal, S., Imhof, T., Koch, M., Nagata, K., Paulsson, M., Zaucke, F., Baumann, U., and Sengle, G. (2020). New specific HSP47 functions in collagen subfamily chaperoning. FASEB J. Published online July 27, 2020. https://doi.org/10.1096/fj.202000570R.
24. Bräuer, P., Parker, J.L., Gerondopoulos, A., Zimmermann, I., Seeger, M.A., Barr, F.A., and Newstead, S. (2019). Structural basis for pH-dependent retrieval of ER proteins from the Golgi by the KDEL receptor. Science *363*, 1103–1107.
25. Feng, L., and Frommer, W.B. (2016). Evolution of Transporters: The Relationship of SWEETs, PQ-loop, and PnuC Transporters. Trends Biochem. Sci. *41*, 118–119.